JOURNAL OF SOLID STATE CHEMISTRY 113, 125–131 (1994)

Synthesis and Crystal Structure of Hollandite-Related Vanadium-Deficient Solid Solution $BaV_{10-x}O_{17}$ ($0.10 \leq x \leq 0.65$)

Yasushi Kanke,[1] Eiji Takayama-Muromachi, Katsuo Kato, and Kousuke Kosuda

National Institute for Research in Inorganic Materials, 1-1 Namiki, Tsukuba, Ibaraki 305, Japan

Received August 11, 1993; in revised form December 6, 1993; accepted December 7, 1993

New vanadium-deficient solid solution, $BaV_{10-x}O_{17}$ ($0.10 \leq x \leq 0.65$), was discovered by an solid state reaction at 1473 K under normal pressure. For $BaV_{9.89}O_{17}$; $M_r = 913.128$, monoclinic, $I2/m$, $a = 10.8130(12)$ Å, $b = 2.9034(1)$ Å, $c = 9.4640(9)$ Å, $\beta = 92.417(5)°$, $V = 296.85(4)$ Å^3, $Z = 1$, $D_x = 5.108$ Mg m^{-3}, $\mu = 10.54$ mm^{-1}, $F(000) = 419.47$, $T = 295$ K, $\lambda(MoK\alpha) = 0.71073$ Å, final $R = 0.040$ for 1158 unique observed reflections. V(1) and V(2) octahedra form a hollandite-type framework. Ba and O(5) atoms alternately occupy and fill up the center of the hollandite-type tunnel. The tunnel accommodates an additional V(3) atom, which is responsible for the vanadium-deficient composition. The V(3) atom forms a coordination octahedron, which distorts the tunnel strongly. Consequently, Ba and O atoms form close-packed layers *chhchh* ··· parallel to (101), of which the *c* layers contain the Ba atoms. The V(3) octahedra neighbor the V(2) octahedra through face-sharing. $BaV_{10-x}O_{17}$ is closely related to the modified vanadium hollandites, $A_{2-x}V_{8+2x}O_{16+x}$ (A = K, Rb), prepared by a high-pressure synthesis.

INTRODUCTION

V^{3+}–V^{4+} mixed-valent oxides are good objects for studying the character of 3*d* electrons, which may be in an intermediate state between localized and itinerant ones. Several vanadium oxide hollandites, $K_2V_8O_{16}$ (1), $K_{2-x}V_8O_{16}$, and $Tl_{2-x}V_8O_{16}$ (2), which contain both V^{3+} and V^{4+}, have been found by high-pressure syntheses. Their V–O coordination octahedra form double chains through edge-sharing and construct a large tunnel in which monovalent cations are located. Abriel *et al.* (3) synthesized, under high pressure, modified-hollandite phases $A_{2-x}V_{8+2x}O_{16+x}$ (A = K, Rb; $x \approx 1$), whose tunnels accommodate not only A cations but also VO_6 octahedra. The crystal structure of $A_{2-x}V_{8+2x}O_{16+x}$ is explained as follows: Approximately half of the A atoms in the ideal hollandite phase, $A_2V_8O_{16}$, are substituted randomly by O atoms ($A_{2-x}V_8O_{16+x}$). Each replacement O atom generates two octahedral sites which are filled up by V atoms ($A_{2-x}V_{8+2x}O_{16+x}$).

In this study, a new hollandite-related solid solution, $BaV_{10-x}O_{17}$ ($0.10 \leq x \leq 0.65$), was discovered by a normal-pressure synthesis. $BaV_{10-x}O_{17}$ is almost isostructural with $A_{2-x}V_{8+2x}O_{16+x}$, but the Ba/O ratio is fixed and its wide solid-solution range is caused exclusively by the varying occupancy of the V(3) atom located in the tunnel.

EXPERIMENTAL

Single-Crystal Preparation

V_2O_3 was obtained by reducing V_2O_5 (99.9%) in hydrogen at 1073 K. V_2O_4 was prepared by heating an equimolar mixture of V_2O_5 and V_2O_3 in a sealed silica tube at 1273 K for 3 days. $Ba_3V_2O_8$ was obtained by heating a mixture of $BaCO_3$ (99.9%) and V_2O_5 in a 3 : 1 molar ratio at 1473 K for 2 days.

$Ba_3V_2O_8$, V_2O_3, and V_2O_4 were mixed in a 1 : 1.5 : 1 molar ratio. About 1.2 g of the mixture was placed in a platinum capsule, sealed in an evacuated silica tube, and then heated at 1523 K for 59 hr. The product was a mixture of white, brown, and black substances. Hexagonal column-shaped black crystals were selected for a X-ray diffraction study. Weissenberg photographs revealed that the phase crystallizes in a body-centered monoclinic structure, with $a = 10.8$ Å, $b = 2.9$ Å, $c = 9.5$ Å, and $\beta = 92°$. The size of the specimen for the intensity collection was $0.100 \times 0.064 \times 0.056 \times 0.040$ mm (along [010], [100], [001], and [101], respectively).

Crystal Structure Analysis

X-ray single-crystal diffraction data were collected on an Enraf-Nonius CAD4 diffractometer with graphite-monochromatized Mo$K\alpha$ radiation ($\lambda = 0.71073$ Å) by a $\omega - \theta$ scan with $\Delta\omega = (0.8 + 0.35 \times \tan\theta)°$ at 295 K. Lattice parameters were determined from 22 reflections ($85° < 2\theta < 90°$). Both ($-21 \leq h \leq 21$, $0 \leq k \leq 5$, $-18 \leq l \leq 0$) and ($-21 \leq h \leq 21$, $-5 \leq k \leq 0$, $0 \leq l \leq 18$)

[1] To whom correspondence should be addressed.

0022-4596/94 $6.00

TABLE 1

Atomic Positions in Wyckoff Notations, Occupancies (g), Positional Parameters, and Equivalent Isotropic Thermal Parameters (Å^2) in $BaV_{9.89}O_{17}$

$$B_{eq} = \tfrac{8}{3}\pi^2 \times (U_{11} + U_{22} + U_{33} + 2U_{13}\cos\beta)$$

Atom	Wyckoff	g	x	y	z	B_{eq}
Ba	2*a*	0.5	0	0	0	1.187(8)
V(1)	4*i*	1	0.86332(4)	0	0.32315(5)	0.464(5)
V(2)	4*i*	1	0.34491(5)	0	0.16375(5)	0.637(6)
V(3)	4*i*	0.4725	0.83507(9)	0	0.01978(11)	0.54(1)
O(1)	4*i*	1	0.6696(2)	0	0.3225(2)	0.53(3)
O(2)	4*i*	1	0.6435(2)	0	0.0392(2)	0.48(2)
O(3)	4*i*	1	0.2890(2)	0	0.3629(2)	0.55(3)
O(4)	4*i*	1	0.0340(2)	0	0.3029(3)	0.65(3)
O(5)[a]	2*a*	0.5	0	0	0	1.187

[a] Refinable parameters are fixed to the corresponding parameters of Ba.

reflections with $0 < 2\theta < 90°$ were measured. Among the collected 2840 reflections, 324 were unobserved. The observed 2516 reflections were averaged into 1378 unique reflections with an R_{int} for F of 0.010. Finally, 1158 reflections with $I > 3\sigma(I)$ were used for refinement. Three standard reflections 600, $0\bar{2}0$, and 006 were measured every 4 hr, and the decrease of intensity was 1.0% during the total exposure time of 202.1 hr. A linear decay correction was applied. Absorption correction was applied with a correction factor for F from 1.190 to 1.809. Structure models were derived with the help of the Patterson function. Atomic scattering factors ($f = f_0 + \Delta f' + i\Delta f''$) for neutral atoms were based on Ref. (4). Structural parameters were refined by a least-squares method (5) based on F, employing an extinction correction.[2] Three possible space groups, *I*2/*m*, *I*2, and *Im*, were examined using an unaveraged 2109 reflections with $I > 3\sigma(I)$. The *I*2/*m* model was successful. Both models of *I*2 provided negative equivalent isotropic thermal parameters for an oxygen site, and some refinable parameters of both models of *Im* did not converge. Therefore, the highest symmetry, *I*2/*m*, was selected among three possible space groups. $R = 0.040$, $R_w = 0.066$, $w = 1/\sigma^2(F)$, $\Delta/\sigma < 0.005$ in final refinement cycle, $-4.10 \le \Delta\rho \le 6.87$ eÅ^{-3}. The atomic fractional coordinates and the equivalent isotropic thermal parameters are listed in Table 1. The anisotropic thermal parameters are listed in Table 2.

[2] See NAPS document No. 05152 for 6 pages of supplementary material. Order from ASIS/NAPS. Microfiche Publications, P.O. Box 3513, Grand Central Station, New York, NY 10163. Remit in advance $4.00 for microfiche copy or for photocopy, $7.75 up to 20 pages plus $.30 for each additional page. All orders must be prepaid. Institutions and Organizations may order by purchase order. However, there is a billing and handling charge for this service of $15. Foreign orders add $4.50 for postage and handling, for the first 20 pages, and $1.00 for additional 10 pages of material, $1.50 for postage of any microfiche orders.

Composition

Because preliminary synthetical studies, coupled with X-ray powder diffraction, had shown that the present phase has a homogeneity range with respect to the V/Ba ratio, the V/Ba ratio of the specimen, 9.89(2), was determined in the early stage of the structure analysis by an X-ray microanalysis using $LaVO_4$ and $BaAl_2O_4$ as standard materials. On the other hand, the structure model in this stage contained four independent O atoms and thus possessed a composition of $BaV_{10}O_{16}$ ($Z = 1$). These results suggest a real composition of $BaV_{9.89}O_{16}$. A preliminary phase-equilibrium study at 1473 K showed, however, that there is a tie line between $Ba_3V_2O_8$ and V_2O_3, and that the present phase appears in the oxygen-rich side of this tie line. Because the composition $BaV_{9.89}O_{16}$ lies in the opposite side of the tie line, the structure model has to contain an additional oxygen atom. The only possible site for this oxygen atom, O(5), is the vacant half of the 2*a* position whose other half is occupied by Ba atoms. The composition becomes $BaV_{9.89}O_{17}$, conforming to the results of the thermogravimetric analyses mentioned below. Though X-ray diffraction cannot distinguish an O atom from a vacant Ba site, the existence of the O(5) is convincing from the following crystal-chemical points of view. Without the O(5), the V(3) site would have a tetragonal-pyramidal fivefold coordination which is unusual for a V^{3+} or V^{4+} ion, and a V(3) cation would have to directly confront another V(3) cation. The O(5) atom completes the octahedral coordination of the V(3) site with an acceptable V(3)–O(5) distance (Table 3). Raw mixtures corresponding to a vanadium-deficient $BaV_{10-x}O_{17}$ model yielded single-phase products with a wide x range as mentioned below, whereas none of the raw mixtures for barium-deficient, oxygen-deficient, or $Ba_{2-x}V_{8+2x}O_{16+x}$

TABLE 2

Anisotropic Thermal Parameters in $BaV_{9.89}O_{17}$

Atom	U_{11}	U_{22}	U_{33}	U_{12}	U_{13}	U_{23}
Ba	0.0151(2)	0.0223(3)	0.00779(14)	0	0.00052(7)	0
V(1)	0.00820(14)	0.0051(2)	0.00436(12)	0	0.00013(6)	0
V(2)	0.00798(14)	0.0060(2)	0.0107(2)	0	0.00270(7)	0
V(3)	0.0055(3)	0.0082(3)	0.0067(3)	0	0.00024(12)	0
O(1)	0.0054(6)	0.0079(7)	0.0070(6)	0	0.0001(3)	0
O(2)	0.0078(6)	0.0051(7)	0.0053(6)	0	−0.0001(3)	0
O(3)	0.0054(6)	0.0083(7)	0.0072(6)	0	0.0004(3)	0
O(4)	0.0047(6)	0.0066(7)	0.0133(8)	0	−0.0009(3)	0
O(5)[a]	U_{11}(Ba)	U_{22}(Ba)	U_{33}(Ba)	0	U_{13}(Ba)	0

[a] Refinable parameters are fixed to the corresponding parameters of Ba.

TABLE 3
Interatomic Distances (Å) in $BaV_{9.89}O_{17}$

Bond	Distance	Bond	Distance
V(1)–O(4)^{i}	1.864(2)	V(3)–O(5)^{i}	1.8010(10)
O(1)	2.094(2)	O(2)	2.088(2)
O(2)^{ii,iii}	1.9542(15)	O(1)^{ii,iii}	2.084(2)
O(1)^{ii,iii}	2.023(2)	O(3)^{vii,viii}	2.120(2)
V(1)–O	1.985	V(3)–O	2.050
V(2)–O(2)^{iv}	1.930(2)	Ba^{ix}–O(4)^{ix,x}	2.875(2)
O(3)	2.004(2)	O(5)^{i,xi}	2.9034(1)
O(4)^{v,vi}	1.9714(15)	O(1)^{iii,viii,xii,xiii}	2.924(2)
O(3)^{v,vi}	2.058(2)	O(3)^{iii,viii,xiii,xiv}	2.957(2)
V(2)–O	1.999	Ba–O	2.923

Note. Symmetry operations: (i) $1 + x, y, z$; (ii) $3/2 - x, 1/2 + y, 1/2 - z$; (iii) $3/2 - x, -1/2 + y, 1/2 - z$; (iv) $1 - x, y, -z$; (v) $1/2 - x, 1/2 + y, 1/2 - z$; (vi) $1/2 - x, -1/2 + y, 1/2 - z$; (vii) $1/2 + x, 1/2 + y, -1/2 + z$; (viii) $1/2 + x, -1/2 + y, -1/2 + z$; (ix) $1 + x, -1 + y, z$; (x) $1 - x, -1 + y, -z$; (xi) $1 + x, -2 + y, z$; (xii) $3/2 - x, -3/2 + y, 1/2 - z$; (xiii) $1/2 + x, -3/2 + y, -1/2 + z$; (xiv) $3/2 - x, -3/2 + y, 1/2 - z$.

models gave a single-phase sample. Therefore, the composition of the present phase was established to be $BaV_{10-x}O_{17}$, and the composition of the single-crystal specimen to be $BaV_{9.89}O_{17}$.

$Ba_3V_2O_8$, V_2O_3, and V_2O_4 were mixed in a $1:(13 - 6x):(1 + 4.5x)$ molar ratio. About 1.5 g of the mixture was placed in a platinum capsule, sealed in an evacuated silica tube, and then heated at 1473 K for 1 day. After cooled to room temperature, the product was ground and examined by X-ray powder diffraction with Cu$K\alpha$ radiation. This procedure was repeated until its X-ray powder pattern changed no longer. One heating run was enough to reach equilibrium. The samples with $0.10 \leq x \leq 0.65$ were single-phase, whereas the samples with both $x = 0.05$ and 0.70 were multiphases (Fig. 1). Therefore, the x range of $BaV_{10-x}O_{17}$ was determined to be $0.10 \leq x \leq 0.65$. The X-ray powder diffraction pattern of $BaV_{9.60}O_{17}$ is listed in Table 4.

To confirm the existence of the O(5) atom, thermogravimetric analyses were performed on single-phase samples with $x = 0.10$, 0.40, and 0.65, using a Perkin–Elmer TGA7 analyzer. About 100 mg of each powdered sample, "$BaV_{9.90}O_y$," "$BaV_{9.60}O_y$," and "$BaV_{9.35}O_y$," was heated from room temperature to 873 K at a rate of 10°/min and kept at 873 K in a flowing oxygen atmosphere. The weight of each sample began to increase above ca. 573 K and became constant within 30 min after reaching 873 K. The oxygen composition for the samples were determined on the assumption that the final valence of V is 5+. The y values for each sample were 17.16 ($x = 0.10$), 17.12 ($x = 0.40$), and 17.12 ($x = 0.65$), which confirm both the existence of the O(5) atom and the composition $BaV_{10-x}O_{17}$.

DISCUSSION

Interatomic distances in $BaV_{9.89}O_{17}$ are shown in Table 3. Figure 2 shows the crystal structure of $BaV_{9.89}O_{17}$ along [010]. V(1) octahedra, as well as V(2) octahedra, form a double chain along [010] through edge-sharing. The double chains enclose a large tunnel along [010]. Adjacent V(1) and V(2) share an octahedral corner. The V(1), V(2)–O framework is analogous to those of hollandite (6).

Ba and O(5) atoms fill up the 2*a* position, which is located at the center of the tunnel. The occupancies of the two atoms are equal (1/2). The V(3) site is situated at a 4*i* position in the tunnel whose occupancy, g, varies widely ($1.35/4 \leq g \leq 1.90/4$). The Ba/O(5) site neighbors two V(3) sites, and the y coordinates of the three sites are equal. The distance between a V(3) site and the adjacent Ba/O(5) site, 1.8010(7) Å (Table 3) is so short that the former cannot be occupied unless the latter accommodates an O atom (Fig. 3). Consequently, half of the V(3) sites are forbidden. More than half (1.35/2–1.90/2) of the

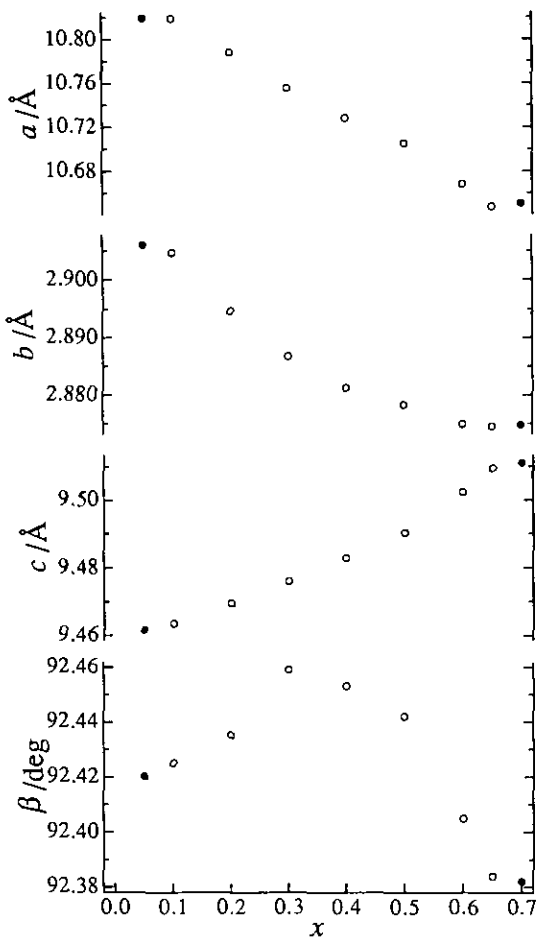

FIG. 1. Lattice parameters versus x for $BaV_{10-x}O_{17}$. Open and filled circles indicate single-phase and multiphase regions, respectively.

TABLE 4
X-Ray Powder Diffraction Pattern of $BaV_{9.60}O_{17}$, Monoclinic, $I2/m$, a = 10.7281(4) Å, b = 2.8812(2) Å, c = 9.4829(4) Å, β = 92.453(4)°

h	k	l	d_{obs}/Å	d_{calc}/Å	I/I_0	h	k	l	d_{obs}/Å	d_{calc}/Å	I/I_0
1	0	1	6.931	6.952	5	4	1	1	1.9098	1.9095	6
2	0	0	5.351	5.359	9	1	0	−5	1.8801	1.8798	3
0	0	2	4.729	4.737	7	1	0	5	1.8522	1.8524	3
2	0	−2	3.627	3.627	7	4	0	−4	1.8139	1.8136	6
2	0	2	3.475	3.476	43	1	1	4	1.7936	1.7938	37
3	0	−1	3.390	3.391	17	6	0	0	1.7867	1.7864	24
3	0	1	3.296	3.297	98	4	0	4	1.7383	1.7381	14
1	0	−3	3.064	3.065	100	3	0	−5	1.7048	1.7045	5
1	0	3	2.994	2.995	97	3	1	−4	1.6511	1.6508	2
1	1	0	2.7823	2.7824	7	3	0	5	1.6454	1.6451	6
0	1	1	2.7563	2.7566	10	5	1	−2	1.6374	1.6347	2
4	0	0	2.6798	2.6796	17	3	1	4	1.6071	1.6071	2
2	1	−1	2.4638	2.4638	11	5	1	2	1.5992	1.5991	27
2	1	1	2.4389	2.4390	31	0	0	6	1.5792	1.5790	27
3	0	−3	2.4110	2.4181	15	2	1	−5	1.5334	1.5333	6
1	1	−2	2.4110	2.4109	15	6	1	−1	1.5076	1.5077	13
1	1	2	2.3880	2.3876	5	2	1	5	1.5036	1.5038	6
4	0	−2	2.3770	2.3763	18	7	0	1	1.5036	1.5015	6
3	0	3	2.3191	2.3175	2	6	0	−4	1.4567	1.4565	1
4	0	2	2.2906	2.2907	11	5	0	−5	1.4509	1.4509	3
3	1	0	2.2429	2.2428	20	0	2	0	1.4406	1.4406	8
2	0	−4	2.2019	2.2015	13	5	1	−4	1.4151	1.4150	22
2	0	4	2.1288	2.1329	32	7	0	−3	1.4015	1.4015	5
0	1	3	2.1288	2.1285	32	5	0	5	1.3904	1.3905	1
5	0	−1	2.1105	2.1103	17	4	0	−6	1.3870	1.3866	1
5	0	1	2.0721	2.0718	2	1	1	−6	1.3798	1.3799	1
3	1	−2	2.0489	2.0485	3	5	1	4	1.3693	1.3695	3
3	1	2	2.0069	2.0063	1	1	1	6	1.3664	1.3668	2
2	1	3	1.9598	1.9589	2	7	0	3	1.3550	1.3552	14
4	1	−1	1.9331	1.9335	6	6	1	3	1.3491	1.3493	5

available V(3) sites are occupied; that is, there is no O(5) atom whose neighboring V(3) sites are both vacant. The O(5) atom bonds to a 1.35–1.90 number of V(3) atom. To minimize electrostatic repulsion, Ba and O atoms must occupy the Ba/O(5) site alternately (Fig. 3). If such an ordered occupation take place, the lattice parameter b should be doubled. Indeed, an oscillation photograph showed diffuse streaks which correspond to $2b$. However, no superlattice reflection was detected in a long-exposure Weissenberg 1/2-layer photograph. That is, the ordering of Ba and O(5) is maintained within a tunnel, whereas there is no such correlation among tunnels. The intratunnel ordering and intertunnel disordering are common to the positions of the Ba atoms in hollandite (7).

$BaV_{10-x}O_{17}$ is almost isostructural with $A_{2-x}V_{8+2x}O_{16+x}$ (A = K, Rb; $x \approx 1$) (3); however, the structures of them are distinguishable in two ways: (i) The A/O(5) ratio of the latter is variable and less than 1, in contrast to the fixed Ba/O(5) ratio (=1) of the former. That is, in the latter, the configuration of A and O(5) is disordered even in a tunnel. (ii) Every pair of the V(3) sites in the latter is occupied perfectly, which neighbors the O(5) atom, whereas some of the corresponding V(3) sites are vacant in the former. Different valences of Ba^{2+} and A^{+} may explain these two points. The electrostatic force between Ba^{2+} and O^{2-} is strong enough to let the Ba and O(5) sites be ordered within a tunnel; on the other hand, the force between A^{+} and O^{2-} is not strong enough. All of the

TABLE 4—*Continued*

h	k	l	d_{obs}/Å	d_{calc}/Å	I/I_0	h	k	l	d_{obs}/Å	d_{calc}/Å	I/I_0
4	1	5	1.3421	1.3422	6	4	0	−8	1.1007	1.1008	2
1	0	7	1.3357	1.3357	5	1	1	−8	1.0940	1.0941	1
4	0	6	1.3357	1.3356	5	9	1	−2	1.0815	1.0815	<1
3	2	1	1.3200	1.3201	1	10	0	0	1.0716	1.0718	1
1	2	−3	1.3040	1.3038	2	4	0	8	1.0663	1.0665	1
1	2	3	1.2983	1.2982	2	0	2	6	1.0642	1.0643	3
3	0	−7	1.2839	1.2840	2	9	1	2	1.0628	1.0628	1
3	1	6	1.2750	1.2751	4	3	1	−8	1.0590	1.0591	1
8	0	2	1.2750	1.2750	4	10	0	−2	1.0554	1.0552	1
4	2	0	1.2689	1.2689	1	1	0	−9	1.0521	1.0520	2
3	0	7	1.2481	1.2481	5	1	0	9	1.0434	1.0433	1
3	2	−3	1.2378	1.2376	1	7	2	1	1.0397	1.0395	1
4	2	−2	1.2318	1.2319	1	6	1	−7	1.0291	1.0291	2
0	1	7	1.2251	1.2250	2	9	1	−4	1.0135	1.0136	1
6	0	−6	1.2089	1.2091	1	7	1	6	1.0084	1.0084	2
2	1	−7	1.2046	1.2044	1	7	2	−3	1.0046	1.0046	2
8	1	1	1.1991	1.1991	1	8	0	6	1.0008	1.0007	1
8	0	−4	1.1882	1.1881	1	4	2	−6	0.9989	0.9990	1
2	1	7	1.1842	1.1843	5	7	2	3	0.9872	0.9871	2
9	0	1	1.1754	1.1754	1	9	1	4	0.9833	0.9834	1
5	0	−7	1.1672	1.1672	2	1	2	7	0.9795	0.9795	1
6	1	5	1.1643	1.1643	3	11	0	−1	0.9736	0.9735	<1
6	0	6	1.1587	1.1588	15	11	0	1	0.9652	0.9651	1
8	1	−3	1.1489	1.1489	1	5	1	8	0.9601	0.9601	2
2	0	8	1.1460	1.1461	1	2	0	10	0.9262	0.9262	1
4	1	−7	1.1306	1.1308	1	6	2	6	0.9029	0.9029	3
6	2	0	1.1212	1.1214	3	11	1	2	0.8992	0.8992	3
8	1	3	1.1194	1.1194	1	1	1	10	0.8938	0.8938	4

O(1)–O(4) atoms bond to at least three V cations, whereas the O(5) atom bonds to at most two V cations and two Ba/*A* cations. The O(5) atom is electrostatically less stable compared to the other O atoms. In $A_{2-x}V_{8+2x}O_{16+x}$, the O(5) atom must bond to two V(3) atoms to be stable, because a monovalent *A* cation cannot provide sufficient electrostatic force to the O(5) atom. In $BaV_{10-x}O_{17}$, on the other hand, a divalent Ba cation provides a strong enough electrostatic force to the O(5) atom so that the O(5) atom does not have to bond to two V(3) atoms. Abriel and Range (8) have found, $K_{3.46}V_{40.6}O_{68.3}$ ($\approx 4\ A_{2-x}V_{8+2x}O_{16+x}$), by a high-pressure synthesis, whose structure corresponds to an ordered structure of $A_{2-x}V_{8+2x}O_{16+x}$. The tunnel of $K_{3.46}V_{40.6}O_{68.3}$ separates into two types, *K*-rich and O(5)-rich tunnels (8). Even in this case, every O(5) atom bonds to two V(3) atoms, which agrees with above discussion.

Table 5 shows that the *ac* parallelograms of $BaV_{9.89}O_{17}$ and $K_{0.78}V_{10.44}O_{17.22}$, together with corresponding $(0.5a)c$ parallelogram of $K_{3.46}V_{40.6}O_{68.3}$, somewhat deviate from a square, compared with those of $K_2V_8O_{16}$ and hollandite. The deviation is attributed to the distortion of the tunnel. The angles $O(4)^{v}$–$O(2)^{ii}$–$O(4)^{xv}$ in the former three are considerably acuter than those of the others. In $BaV_{10-x}O_{17}$, the difference between *a* and *c* increases with decreasing *x* (Fig. 1). That is, the distortion of the tunnel gets stronger with increasing V(3) occupancy, to provide appropriate V(3)–O distances.

The Ba atoms are coordinated by 12 O atoms. The Ba and O atoms form close packed layers *chhchh* · · · parallel to (101), of which the *c* layers contain the Ba atoms. Depending on *x*, 1.35/4–1.90/4 of the V(2) octahedra neighbor the V(3) octahedra through face-sharing. The close-packed layers and the face-sharing V octahedra are common in V^{3+}–V^{4+} mixed valent oxides. The face-sharing V(2)–$V(3)^{iv}$ distance in $BaV_{9.89}O_{17}$, 2.553(1) Å (Table

TABLE 5
Crystal Systems, Space Groups, Lattice Parameters, Face-Sharing V(2)–V(3)^{iv} Distances, and O(4)^{v}–O(2)^{ii}–O(4)^{xv} Angles in $BaV_{9.89}O_{17}$ and Related Phases

	$BaV_{9.89}O_{17}$	$K_{0.78}V_{10.44}O_{17.22}$	$K_{3.46}V_{40.6}O_{68.3}$[a]	$K_2V_8O_{16}$	Hollandite[b]
Crystal system	Monoclinic	Monoclinic	Monoclinic	Tetragonal	Monoclinic
Space group	*I2/m*	*I2/m*	*C2/m*	*I4/m*	*I2/m*
a (Å)	10.8130(12)	10.979(5)	21.959(12)	9.963(5)	10.026(3)
b (Å)	2.9034(1)	2.922(3)	5.935(7)	2.916(2)	2.8782(7)
c (Å)	9.4640(9)	9.383(5)	9.383(6)	9.963(5)	9.729(3)
β (degrees)	92.417(5)	92.26(4)	92.26(5)	90	91.03(2)
V(2)–V(3)^{iv}	2.553(1)	2.591(4)	2.594(3) 2.670(6)		
O(4)^{v}–O(2)^{ii}–O(4)^{xv}	72.94(5)°	72.08(15)°	72.04(22)° 72.80(26)° 70.77(32)°	90°	84.26(5)°
Ref.	This work	(3)	(8)	(2)	(16)

Note. Symmetry operations: Operations (ii) and (v) are shown in Table 3. (xv) $1/2 + x$, $1/2 + y$, $1/2 + z$.

[a] Cell parameters *a* and *b* correspond to 2*a* and 2*b* of $K_{0.78}V_{10.44}O_{17.22}$, respectively. This phase has two V(3) sites and three V(2), O(2), and O(4) sites.

[b] $(Ba_{0.75}Pb_{0.16}Na_{0.10}K_{0.04})(Mn, Fe, Al)_8(O, OH)_{16}$: Mn is the major element among Mn, Fe, and Al.

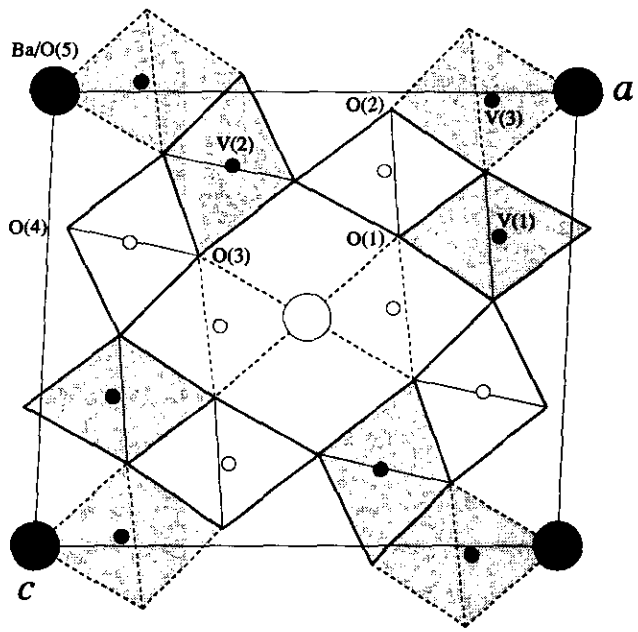

FIG. 2. Projection of the structure of $BaV_{9.89}O_{17}$ onto (010) drawn with ATOMS (Shape Software). Large circles and small circles indicate Ba/O(5) atoms and V atoms, respectively. The *y* coordinates of filled circles are 0, and those of open circles are 1/2. Hatched and open tetragons denote coordination octahedra of V atoms, whose V atoms' *y* coordinates are 0 and 1/2, respectively. The V(3) site is a vanadium-deficient site so that its coordination octahedra are expressed by broken lines.

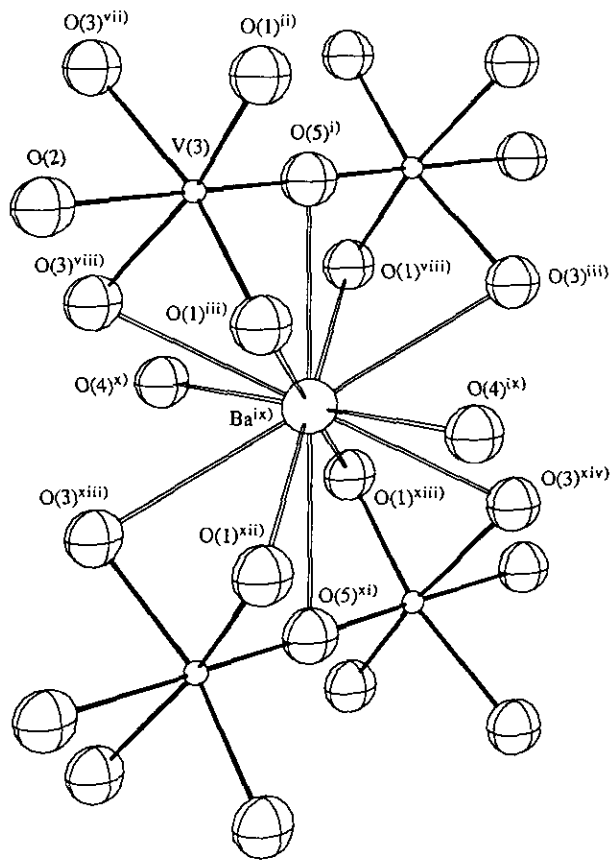

FIG. 3 Coordinations of V(3) and Ba atoms drawn with ORTEP II (14) in FAT-RIETAN (15). Symmetry operations are listed in Table 3.

TABLE 6
Bond Valence Sum in $BaV_{9.89}O_{17}$

Site assumed valence	V(1)		V(2)		V(3)	
	+3	+4	+3	+4	+3	+4
$BaV_{9.89}O_{17}$	+3.177	+3.549	+3.030	+3.385	+2.766	+3.090
$K_{0.78}V_{10.44}O_{17.22}$	+3.117	+3.482	+2.924	+3.266	+2.738	+3.059
$K_{3.46}V_{40.6}O_{68.3}$[a]	+3.127	+3.494	+2.747	+3.068	+2.832	+3.164
	+2.900	+3.240	+2.880	+3.218		
	+3.070	+3.430	+2.851	+3.185	+2.680	+2.994
$K_2V_8O_{16}$	+3.404	+3.803	+3.404	+3.803		

[a] This phase has three V(1), three V(2), and two V(3) sites. Upper, middle, and lower lines indicate V(*n*1), V(*n*2), and V(*n*3) sites (8), respectively.

5), is the shortest among those in $K_{0.78}V_{10.44}O_{17.22}$ (2.591(4) Å, Table 5), $K_{3.46}V_{40.6}O_{68.3}$ (2.594(3) and 2.670(6) Å, Table 5), V_3O_5 (2.7632(4) and 2.8171(4) Å (9)), NaV_6O_{11} (2.6840(4) Å (10)), SrV_6O_{11} (2.721(3) Å (10)), and $NaFe_3V_9O_{19}$ (2.587(6) Å (11)).

Abriel and Range (8) discussed V^{3+}–V^{4+} distribution in $A_{2-x}V_{8+2x}O_{16+x}$ phases on the basis of mean V–O distance and the deviation of each V–O bond length from ideal V^{3+}–O^{2-} or V^{4+}–O^{2-} distances. They concluded that the V(2) sites are occupied by V^{3+} and the others by both V^{3+} and V^{4+} in $A_{2-x}V_{8+2x}O_{16+x}$ phases, and that the V(1) sites of $K_{3.46}V_{40.6}O_{68.3}$ split into three types: V^{3+}, mixed-valent V, and V^{4+} sites. On the other hand, our bond valence sum (12) calculation for $BaV_{9.89}O_{17}$ and $K_{0.78}V_{10.44}O_{17.22}$ suggests that the V(3) sites are occupied by V^{3+} and the others by both V^{3+} and V^{4+} (Table 6). Indeed, in $BaV_{9.89}O_{17}$, $\overline{V(3)\text{–}O}$ is consistent with $r(^{VI}V^{3+}) + r(^{IV}O^{2-}) = 2.02$ Å (13), and both $\overline{V(1)\text{–}O}$ and $\overline{V(2)\text{–}O}$ (Table 3) are between $r(^{VI}V^{3+}) + r(^{IV}O^{2-})$ and $r(^{VI}V^{4+}) + r(^{IV}O^{2-}) = 1.96$ Å (13). In $K_{3.46}V_{40.6}O_{68.3}$, the V(1) site appears to accommodate both V^{3+} and V^{4+}; however, the V(2) and V(3) sites appear to split into V^{3+} sites (V(21) and V(33)) and mixed-valent V sites (Table 6).

ACKNOWLEDGMENTS

One of the authors (Y.K.) is grateful to Dr. Yuichi Michiue of NIRIM for the information about vanadium oxide hollandites and to Dr. Fujio Izumi of NIRIM for his help with using ORTEP II (14) in FAT-RIETAN (15).

REFERENCES

1. H. Okada, N. Kinomura, S. Kume, and M. Koizumi, *Mater. Res. Bull.* **13,** 1047 (1978).
2. W. Abriel, F. Rau, and K.-J. Range, *Mater. Res. Bull.* **14,** 1063 (1979).
3. W. Abriel, C. Garbe, F. Rau, and K.-J. Range, *Z. Kristallogr.* **176,** 113 (1986).
4. "International Tables For X-Ray Crystallography," Vol. IV. Kynoch Press, Birmingham (present distributor: Kluwer Academic, Dordrecht), 1974.
5. B. A. Frenz & Associates Inc., "SDP Structure Determination Package," 4th ed. College Station, TX, 1985, and Enraf-Nonius, Delft, Holland, 1981.
6. A. Byström and A. M. Byström, *Acta Crystallogr.* **3,** 146 (1950).
7. A. Bryström and A. M. Byström, *Acta Crystallogr.* **4,** 469 (1951).
8. W. Abriel and K.-J. Range, *Z. Kristallogr.* **178,** 225 (1987).
9. S. Åsbrink, *Acta Crystallogr. Sect. B* **36,** 1332 (1980).
10. Y. Kanke, K. Kato, E. Takayama-Muromachi, and M. Isobe, *Acta Crystallogr. Sect. C* **48,** 1376 (1992).
11. Y. Kanke, F. Izumi, Y. Morii, S. Funahashi, and K. Kato, *J. Solid State. Chem.* **104,** 319 (1993).
12. I. D. Brown and D. Altermatt, *Acta Crystallogr. Sect. B* **41,** 244 (1985).
13. R. D. Shannon, *Acta Crystallogr. Sect. A* **32,** 751 (1976).
14. C. K. Johnson, ORTEP II. Report ORNL-5138, Oak Ridge National Laboratory, TN, 1976.
15. F. Izumi, *in* "The Rietveld Method" (R. A. Young, Ed.), Chap. 13. Oxford Univ. Press, London, 1993.
16. J. E. Post, R. B. von Dreele, and P. R. Buseck, *Acta Crystallogr. Sect. B* **38,** 1056 (1982).